Clinical Neurophysiology 130 (2019) 1446–1454

Contents lists available at ScienceDirect

Clinical Neurophysiology

journal homepage: www.elsevier.com/locate/clinph

Spatiotemporal dynamics of auditory and picture naming-related high-gamma modulations: A study of Japanese-speaking patients

Naoki Ikegaya [a,b,1], Hirotaka Motoi [c,d,1], Keiya Iijima [a], Yutaro Takayama [a,b], Toshimune Kambara [d,g], Ayaka Sugiura [d], Brian H. Silverstein [f], Masaki Iwasaki [a,*,2], Eishi Asano [d,e,*,2]

[a] Department of Neurosurgery, National Center Hospital, National Center of Neurology and Psychiatry, Tokyo 1878551, Japan
[b] Department of Neurosurgery, Graduate School of Medicine, Yokohama City University, Yokohama 2360004, Japan
[c] Department of Pediatrics, Graduate School of Medicine, Yokohama City University, Yokohama 2360004, Japan
[d] Department of Pediatrics, Wayne State University, Children's Hospital of Michigan, Detroit, MI 48201, USA
[e] Department of Neurology, Wayne State University, Children's Hospital of Michigan, Detroit, MI 48201, USA
[f] Translational Neuroscience Program, Wayne State University, Detroit, MI 48202, USA
[g] Department of Psychology, Hiroshima University, Hiroshima 7398524, Japan

See Editorial, pages 1403–1404

ARTICLE INFO

Article history:
Accepted 15 April 2019
Available online 22 April 2019

Keywords:
High-frequency oscillations (HFOs)
Ripples
Event-related high-gamma activity
Epilepsy surgery
Intracranial EEG recording
Functional brain mapping

HIGHLIGHTS

- Picture naming-specific high-gamma augmentation was noted in the bilateral occipital-fusiform pathways.
- Auditory naming-specific high-gamma augmentation was noted in the bilateral superior temporal gyrus.
- Auditory naming-specific high-gamma augmentation was noted in the left perisylvian network regions.

ABSTRACT

Objective: To characterize the spatiotemporal dynamics of auditory and picture naming-related cortical activation in Japanese-speaking patients.
Methods: Ten patients were assigned auditory naming and picture naming tasks during extraoperative intracranial EEG recording in a tertiary epilepsy center. Time-frequency analysis determined at what electrode sites and at what time windows during each task the amplitude of high-gamma activity (65–95 Hz) was modulated.
Results: The superior-temporal gyrus on each hemisphere showed high-gamma augmentation during sentence listening, whereas the left middle-temporal and inferior-frontal gyri showed high-gamma augmentation peaking around stimulus offset. Auditory naming-specific high-gamma augmentation was noted in the bilateral superior-temporal gyri as well as left frontal-parietal-temporal perisylvian network regions, whereas picture naming-specific augmentation was noted in the occipital-fusiform regions, bilaterally. The inferior pre- and postcentral gyri on each hemisphere showed modality-common high-gamma augmentation time-locked to overt responses.
Conclusions: The spatiotemporal dynamics of auditory and picture naming-related high-gamma augmentation in Japanese-speaking patients were qualitatively similar to those previously reported in studies of English-speaking patients.

Abbreviations: STG, superior temporal gyrus; MTG, middle temporal gyrus; ITG, inferior temporal gyrus; SMG, supramarginal gyrus; IFG, inferior frontal gyrus; iPreCG, inferior precentral gyrus; iPostCG, inferior postcentral gyrus; ESM, electrical stimulation mapping; fMRI, functional MRI; iEEG, intracranial EEG.

* Corresponding authors at: Department of Neurosurgery, National Center Hospital, National Center of Neurology and Psychiatry, 4-1-1 Ogawahigashi-Cho, Kodaira, Tokyo 187-8551, Japan (M. Iwasaki). Department of Neurodiagnostics, Children's Hospital of Michigan, Wayne State University, 3901 Beaubien St., Detroit, MI 48201, USA (E. Asano).
E-mail addresses: iwa@ncnp.go.jp (M. Iwasaki), easano@med.wayne.edu (E. Asano).

[1] N. I. and H. M. share first authorship.
[2] E. A. and M. I. share senior authorship.

https://doi.org/10.1016/j.clinph.2019.04.008

Significance: The cortical dynamics for auditory sentence recognition are at least partly shared by cohorts speaking two distinct languages. Multicenter studies regarding the clinical utility of high-gamma language mapping across Eastern and Western hemispheres may be feasible.

1. Introduction

Regardless of patient demographics, the goals of resective epilepsy surgery include the minimization of postoperative functional deficit risk. Electrical stimulation mapping (ESM) and functional MRI (fMRI), with anatomical landmarks taken into consideration, can effectively estimate the locations of language areas during presurgical evaluation (Lesser et al., 2010; Austermuehle et al., 2017). A growing number of investigators currently employ measurement of task-related high-gamma activity at ≥50 Hz on intracranial EEG (iEEG) recording as a complementary tool for language mapping (Towle et al., 2008; Crone et al., 2011; Ruescher et al., 2013; Mooij et al., 2016; Arya et al., 2018). Task-related augmentation of high-gamma activity is an excellent summary measure of task-related cortical activation (Ray et al., 2008; Keller et al., 2013). High-gamma language mapping is useful not only to localize areas that support language function but also to clarify the temporal order of task-related cortical activation (Cervenka et al., 2013; Nakai et al., 2017). Picture naming is the task most commonly employed in high-gamma language mapping, partly because of its simplicity of the task design (Arya et al., 2018). Based on previous iEEG studies, the spatiotemporal dynamics of high-gamma augmentation during picture naming are qualitatively similar across patients speaking distinct native languages, including Japanese (Tanji et al., 2005; Kunii et al., 2013; Ogawa et al., 2017), Chinese (Lin et al., 2015; Wen et al., 2017), English (Sinai et al., 2005; Edwards et al., 2010; Cervenka et al., 2013; Arya et al., 2017; Babajani-Feremi et al., 2018; Forseth et al., 2018; Nakai et al., 2019), French (Lachaux et al., 2007; Llorens et al., 2011), and Dutch (Bauer et al., 2013). Picture naming-related high-gamma augmentation was reported to take place commonly in the bilateral occipital and fusiform regions immediately following stimulus presentation, subsequently involve left inferior frontal gyrus (IFG), and finally involve the bilateral inferior pre- (iPreCG) and postcentral gyri (iPostCG) during overt responses (Forseth et al., 2018; Nakai et al., 2019).

Auditory description naming, in which patients answer auditory sentence questions, is also a useful task to localize language areas (Hamberger and Seidel, 2003). Previous iEEG studies using auditory sentence stimuli in English have demonstrated high-gamma augmentation bilaterally in the superior temporal gyrus (STG) and iPreCG shortly after stimulus onset, then spreading in the left perisylvian network regions including middle temporal (MTG), supramarginal gyrus (SMG), and IFG peaking around the offset of sentence stimuli, and eventually in the bilateral iPreCG, iPostCG, and STG during an overt answer (Nakai et al., 2017; Forseth et al., 2018). Building from these English-language data, we then asked, *Are the spatiotemporal dynamics of high-gamma augmentation during auditory description naming grossly similar across patients speaking different languages?* Empirical data from non-English speaking patients are currently scarce, but we expected that this study of Japanese speaking patients would adequately address this question. Japanese is different from English in a number of aspects including syntax, morphology, lexis, and phonology.

The purpose of this iEEG study was to investigate the hypothesis that the spatiotemporal dynamics of naming-related high-gamma augmentation in Japanese-speaking patients would be qualitatively similar to those reported in studies of English-speaking patients. We specifically hypothesized that auditory naming-related high-gamma augmentation in the left frontal-parietal-temporal perisylvian network regions, herein defined to consist of left MTG, SMG, and IFG (Binder et al., 1997; Hickok and Poeppel, 2007; Xiang et al., 2010), would peak around the offset of sentence stimuli rather than at the offset of each word. This hypothesis was motivated by the notion that the human brain largely processes the meaning of an entire sentence question as a single chunk rather than processing each word strictly in a piece-by-piece manner (Wickens, 1970; Baddeley, 2000) and that distant areas within the left frontal-parietal-temporal perisylvian network regions are anatomically and functionally connected (Matsumoto et al., 2004; 2012; Catani and Mesulam, 2008; Martino et al., 2013). Based on previous observations in English-speaking patients (Nakai et al., 2019), we hypothesized that picture naming-specific high-gamma augmentation would be noted in the bilateral ventral visual pathways including the occipital and fusiform regions, whereas auditory naming-specific high-gamma augmentation would be noted in the bilateral STG as well as in the aforementioned left frontal-parietal-temporal perisylvian network regions. We also discuss potential pitfalls for future multicenter collaborative studies on the clinical utility of high-gamma mapping across Eastern and Western hemispheres.

2. Methods

2.1. Participants

Inclusion criteria consisted of patients who underwent both auditory description naming (Fig. 1A) and picture naming (Fig. 1B) tasks during extraoperative iEEG recording at National Center of Neurology and Psychiatry, Tokyo, Japan. Exclusion criteria consisted of: (i) presence of massive brain malformations deforming the central or lateral sulcus, (ii) inability to complete the tasks, (iii) primary language other than Japanese, (iv) history of previous resective epilepsy surgery, and (v) right-hemispheric language dominance as suggested by the result of Wada test or left-handedness associated with left-hemispheric congenital neocortical lesions (because of the increased likelihood of interhemispheric language reorganization; Kojima et al., 2013a). Ten patients satisfying the inclusion and exclusion criteria were studied (age range: 19–54 years; 5 females; Table 1). None of our patients fluently speak a language other than Japanese. This study (A2017-028) was approved by the Institutional Review Board at the National Center of Neurology and Psychiatry, and performed under the approved guidelines. Informed consent was obtained from the patients or the guardian of a pediatric patient.

2.2. Acquisition of iEEG and 3D MR images

The data acquisition and analytic methods were similar to those reported in previous iEEG studies (Kambara et al., 2018b; Nakai et al., 2019). As part of our routine presurgical evaluation for localization of the epileptogenic zone, platinum electrodes were chronically implanted on the affected hemisphere in the operation room and were used to subsequently record iEEG signals directly from the cerebral cortex in the inpatient ward. The iEEG sampling rate was 1000 Hz (Nihon Kohden EEG 1200, Tokyo, Japan). Across 10

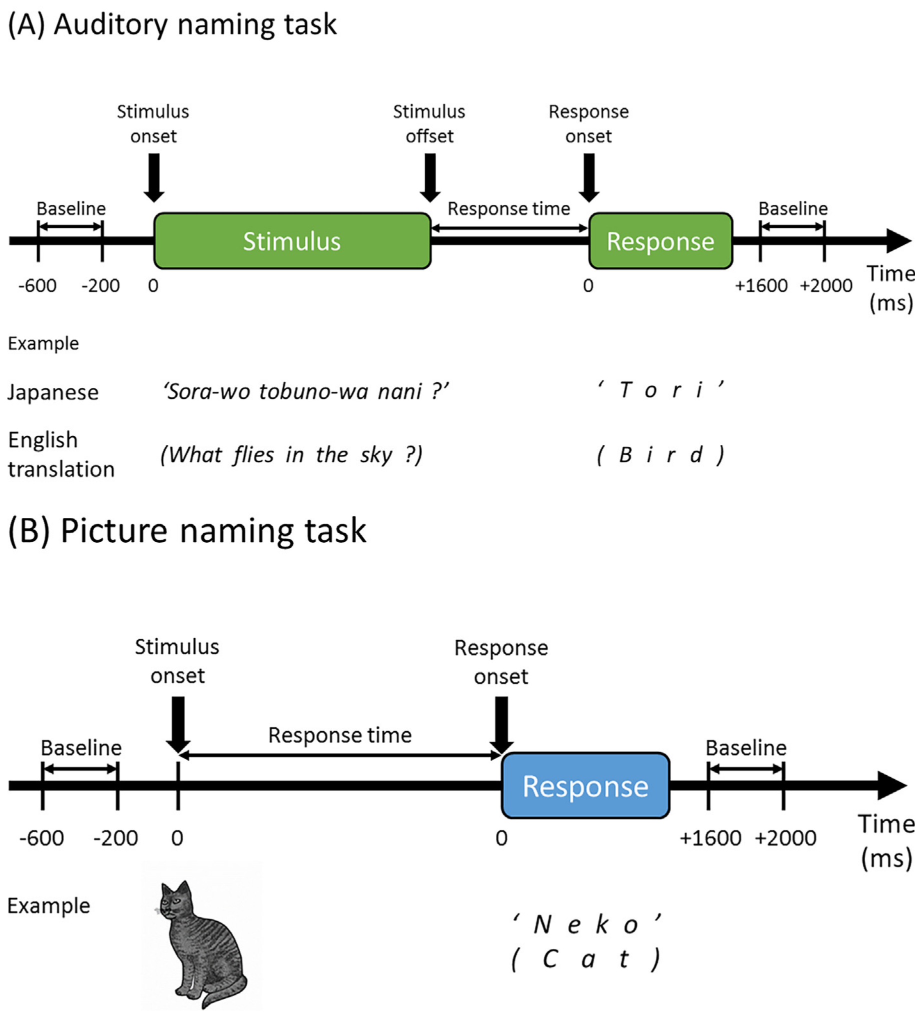

Fig. 1. Auditory and picture naming tasks. (A) Auditory description naming task. The response time was defined as the period between the stimulus offset and the onset of overt response. Each auditory question included the following three chunks: [object or complement], [verb] and [what, when or where]. (B) Picture naming task. The response time was defined as the period between stimulus onset and response onset. At the end of each response, the examiner pressed the button to present the next stimulus following a cross in the center of the screen presented for 2000 or 2500 ms. In both auditory and picture naming tasks, the baseline period was set at a 400-ms silent period between 600 and 200 ms prior to stimulus onset in the analysis time-locked to stimulus onset and a 400-ms silent period between 1600 and 2000 ms following overt response in the analysis time-locked to response onset.

patients, a total of 428 subdural disk electrodes (diameter: 2.3 mm; center-to-center distance: 10 mm) and 402 depth electrodes (length: 370 mm; center-to-center distance: 5 mm) were implanted (number of electrodes per patient: 64–124). iEEG signals were visually evaluated and later quantitatively analyzed using a common average reference (i.e., an average of voltages across all channels except for those showing large interictal epileptiform discharges or artifacts). A 3D cortical surface image with electrode locations was created using a pre-implantation T1-weighted image and a post-implantation CT image as previously reported (Budke et al., 2018). The accuracy of this co-registration procedure was confirmed by a visual assessment of intraoperative photographs and the post-implantation CT image (Nakai et al., 2017).

2.3. Auditory and picture naming tasks

Patients were assigned auditory and picture naming tasks during extraoperative iEEG recording. Tasks were employed at the bedside during wakefulness, and patient participation time was less than 30 minutes in total. During the auditory naming task (Fig. 1A), patients were instructed to overtly verbalize an answer for a series of 1.8 s auditory sentence questions (such as *'Sora-wo tobuno-wa nani?'* [English translation: '*What flies in the sky?*']). A total of 100 prerecorded questions were presented via a speaker. During the picture naming task (Fig. 1B), patients were instructed to overtly name an object presented on an LCD monitor. A total of 60 picture stimuli (such as a cat, desk, etc. [Kojima et al., 2013b]) were presented at the center of a 15-inch laptop computer. The size of pictures ranged from 11 to 16 cm in height and width. Presentation of auditory and picture stimuli was performed with PowerPoint Presentation Software (Microsoft Corporation, Redmond, WA, USA); thereby, the timings of stimulus presentations, overt patient responses, and iEEG signals were synchronized using a photosensor and microphone (Kambara et al., 2018b). Trials not accompanied by overt, correct answers were excluded from subsequent time-frequency analysis (Nakai et al., 2019).

2.4. Time-frequency analysis

We determined the spatiotemporal dynamics of naming-related high-gamma modulations using a time-frequency analysis methodology as previously reported (Brown et al., 2008; Kambara et al., 2018b). Channels showing artifacts on visual assessment were excluded from analysis. iEEG voltage traces were

Table 1
Patient profile.

Total number of patients	10
Mean age (year old)	33.3
Median age (year old)	32.5
Range of age (year old)	19–54
Range of age of epilepsy onset (year old)	5–52
Proportion of female (%)	50.0
Proportion of Right handedness (%)	100.0
Proportion of sampled hemisphere (%)	
Left	5 (50.0)
Right	4 (40.0)
Both	1 (10.0)
Seizure onset zone. Number of patients (%)	
Left frontal	2 (12.5)
Left temporal	3 (18.8)
Left parietal	1 (6.3)
Left lateral occipital	0 (0)
Right frontal	2 (12.5)
Right temporal	4 (25.0)
Right parietal	3 (18.8)
Right lateral occipital	1 (6.3)
Mean number of antiepileptic drugs	2.7
Median number of antiepileptic drugs	2.5
Range of number of antiepileptic drugs	1–5
Carbamazepine	4 (16.0)
Clobazam	1 (4.0)
Clonazepam	2 (8.0)
Diazepam	2 (8.0)
Lacosamide	2 (8.0)
Levetiracetam	4 (16.0)
Lamotrigine	2 (8.0)
Perampanel	1 (4.0)
Phenytoin	1 (4.0)
Topiramate	1 (4.0)
Valproate	3 (12.0)
Zonisamide	2 (8.0)
Etiology. Number of patients (%)	
Tumor	2 (20.0)
Dysplasia	5 (50.0)
Hippocampal sclerosis	1 (10.0)
Arteriovenous malformation	1 (10.0)
Heterotopia	1 (10.0)

aligned to stimulus onset and response onset, and transformed into the time-frequency domain, in steps of 10 ms and 5 Hz, using a complex demodulation technique (Papp and Ktonas, 1977) incorporated in the BESA software package (BESA GmbH, Gräfelfing, Germany; Hoechstetter et al., 2004). This was effectively equivalent to a Gabor transformation since the time-frequency transformation was obtained by multiplication of the time-domain signals with a complex exponential, followed by low-pass filtering consisting of a finite impulse response filter of Gaussian shape. In each 10 ms window, we measured the percent change in high-gamma, defined as 65–95 Hz, amplitude (equivalent to the square root of power) relative to the mean amplitude during a baseline period. The baseline period was defined as a 400-ms quiet, resting period between trials as shown in Fig. 1. The high-gamma frequency range was defined to avoid alternating current artifacts and their harmonics. The frequency of alternating current is 50 Hz in Eastern Japan (including Tokyo) but 60 Hz in Western Japan, thus we chose to avoid both ranges to maximize our ability to relate our findings to data collected from across the region. At each 10-ms 5-Hz time-frequency bin, we determined whether augmentation (or suppression) of high-gamma amplitude reached statistical significance with the studentized bootstrap statistic followed by Simes' correction (Brown et al., 2008; Koga et al., 2011). The aforementioned analyses characterized the temporal dynamics of naming-related high-gamma modulations at each recording channel of each patient (Fig. 2; Supplementary Figs. S1–S9). To rule out spurious high-gamma activity related to EMG artifacts, we repeated the time-frequency analysis with bipolar montage with neighboring electrode pairs, which can reduce the contamination of EMG signals from a distant source (Nagasawa et al., 2011; Kambara et al., 2018b). If overt response-related high-gamma augmentation was seen on the common average reference but not on the bipolar montage, we treated such high-gamma augmentation as derived from EMG artifacts (Forseth et al., 2018).

In Fig. 3, we plotted naming-related high-gamma activity of channels, each of which showed significant high-gamma augmentation during either task. These plots allowed us to determine whether auditory naming-related high-gamma augmentation at left MTG, SMG, and IFG would peak at the offset of sentence stimuli (Fig. 3B, F, and G). Using McNemar's test, we determined whether the bilateral ventral visual pathways, defined to include occipital and fusiform regions, were preferentially associated with picture naming-related high-gamma augmentation. Likewise, we determined whether the bilateral STG as well as the left frontal-parietal-temporal perisylvian network regions, defined to include left MTG, SMG, and IFG, were preferentially associated with auditory naming-related high-gamma augmentation.

3. Results

The median response time (Fig. 1) during auditory naming task ranged from 1132 to 3678 ms (grand median across ten patients: 1922 ms), whereas that during picture naming task ranged from 855 to 2932 ms (grand median: 1246 ms). All ten patients showed significant naming-related high-gamma augmentation during both auditory and picture naming tasks (Fig. 2 and Supplementary Figs. S1–S9).

3.1. Auditory naming-related high-gamma augmentation

Significant high-gamma augmentation was noted in the STG on either hemisphere during the presentation of auditory stimuli, with the largest amplitude augmentation immediately following the sentence onset (average peak latency relative to stimulus onset: +160 ms on left STG and +300 ms on right STG; Fig. 3A). Modest but significant high-gamma augmentation was noted in the left iPreCG during the presentation of auditory stimuli (Fig. 3H). Around stimulus offset, high-gamma augmentation was observed in subsets of the left MTG, SMG, and IFG (average peak latency relative to stimulus offset: −90 ms on left MTG; −680 ms on left SMG; +30 ms on left IFG; Table 2; Fig. 3B, F, and G). Significant high-gamma augmentation then involved the left and right iPreCG and iPostCG with the magnitude of augmentation peaking at the onset of overt responses (Fig. 3H and I). Significant high-gamma augmentation was also observed in the bilateral STG following the onset of overt responses (Fig. 3A).

3.2. Picture naming-related high-gamma augmentation

Significant high-gamma augmentation was noted initially in the left and right occipital lobes and fusiform gyri (Fig. 3D and E). Prior to overt response onset, significant high-gamma augmentation was observed in small subsets of the left MTG and IFG (Table 2), and broadly in the left and right iPreCG and iPostCG. Across response-involved ROIs, the magnitude of high-gamma augmentation peaked at the onset of overt responses (Fig. 3H and I). Significant high-gamma augmentation was also observed in the left and right STG following the onset of overt responses (Fig. 3A).

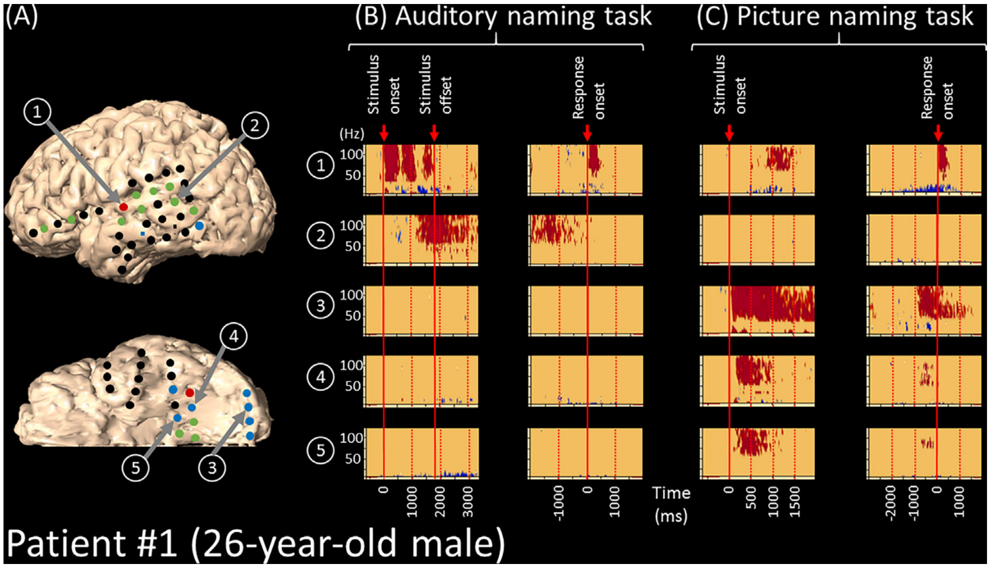

Fig. 2. Naming-related high-gamma modulations in a 26-year-old male (Patient #1). (A) Representative 3D MR surface image from one patient. Circular dots: subdural electrode sites. Square dots: depth electrode insertion site. Red electrodes: Significant high-gamma augmentation during both auditory and picture naming tasks. Green electrodes: Significant high-gamma augmentation during auditory naming task alone. Blue electrodes: Significant high-gamma augmentation during picture naming task alone. Black electrodes: Failure to show significant high-gamma augmentation in either task. (B) Time-frequency plots during the auditory naming task. Red blobs indicate significant relative increase compared to baseline; blue blobs indicate significant relative decrease compared to baseline. Major vertical lines indicate stimulus onsets/offsets and response onsets; minor vertical lines indicate time scale at second intervals. (C) Time-frequency plots during picture naming task. (For interpretation of the references to colour in this figure legend, the reader is referred to the web version of this article.)

3.3. High-gamma modulations specific and common across stimulus modalities

The McNemar's test demonstrated that the bilateral ventral visual pathways were preferentially associated with picture naming-related high-gamma augmentation (p = 0.0001; odds ratio: 11.0 [95%CI: 2.7–96.5]). Specifically, 22 out of 56 channels in the ventral visual pathways showed high-gamma augmentation during the picture naming task alone, whereas only 2 showed high-gamma augmentation during the auditory naming task alone (Table 2).

The McNemar's test demonstrated that the bilateral STG channels were preferentially associated with auditory naming-related high-gamma augmentation (p = 0.0001; odds ratio cannot be computed). Specifically, 26 out of 108 STG channels showed high-gamma augmentation during the auditory naming task alone, whereas none showed high-gamma augmentation during the picture naming task alone (Table 2).

The McNemar's test demonstrated that the left frontal-parietal-temporal perisylvian network regions consisting of left the MTG, SMG, and IFG were preferentially associated with auditory naming-related high-gamma augmentation (p = 0.01; odds ratio: 3.4 [95%CI: 1.2–11.8]). Specifically, 17 out of 134 left perisylvian network channels showed high-gamma augmentation during auditory naming task alone, whereas only 5 showed high-gamma augmentation during picture naming task alone (Table 2).

Overt response-related high-gamma augmentation in the bilateral iPreCG/iPostCG sites was commonly noted during auditory and picture naming tasks. Specifically, 18 out of 38 iPreCG/iPostCG sites showed high-gamma augmentation during both picture and auditory naming tasks, whereas 2 showed augmentation during picture naming task alone and another 2 showed augmentation during auditory naming task alone. The McNemar's test failed to prove that iPreCG/iPostCG sites were preferentially associated with one task over the other (p = 0.6; 95%CI: 1.0 [95%CI: 0.07–13.8]).

A single right IFG site of each of the two patients showed significant high-gamma suppression commonly during the presentation of auditory and picture stimuli (Supplementary Figs. S7 and S9).

4. Discussion

4.1. Summary of our observations

To our knowledge, this is the first ECoG study of high-gamma modulations elicited by an auditory description naming task in Japanese-speaking patients. As of 2018, the United States Department of State has classified Japanese as one of the five 'super-hard' languages exceptionally difficult to learn for native English speakers (https://www.state.gov/m/fsi/sls/c78549.htm). In turn, native Japanese speakers have likewise experienced difficulty studying English in school and ranked 40th out of 48 countries in the Test of English for International Communication (TOEIC) in 2013 (Hongo, 2014). These observations are attributed mainly to a fundamental difference in syntax, phonology, lexic and morphology between two languages (Cook, 2016). For example, a verb typically comes after the object in Japanese but before the object in English (Lehmann, 1973). One has to listen to the very end of the verb, in general, to understand each sentence in Japanese (Teruya, 2006). Nonetheless, the spatiotemporal dynamics of high-gamma amplitude changes in our Japanese-speaking patients were grossly similar to those reported in English-speaking patients (Nakai et al., 2017; Forseth et al., 2018). Our observations are consistent with the hypothesis that the neural dynamics supporting auditory sentence recognition and visual object recognition are grossly shared by individuals speaking two distinct languages.

During sentence listening, stimulus-related high-gamma augmentation in the bilateral STG is thought to support acoustic and phonological processing (Démonet et al., 1992), whereas activity in the iPreCG may be related to phonological processing or verbal working memory maintenance (Nishida et al., 2017; Kambara et al., 2018a). A previous study reported that electrical stimulation of STG on either hemisphere elicited auditory hallucination (Nakai et al., 2017). High-gamma augmentation in the left frontal-parietal-temporal perisylvian network regions is likely associated with semantic processing and lexical retrieval (Binder et al., 1997; Hickok and Poeppel, 2007). Previous studies reported that stimulation of left MTG, SMG, and IFG was associated with increased chance of inducing receptive or expressive dysphasia (Sanai et al., 2008; Tate et al., 2014; Nakai et al., 2017). Overt response-related high-gamma augmentation in the bilateral iPreCG/iPostCG likely reflects neural activation supporting an oral movement. Previous studies reported that stimulation of these regions induced either speech arrest or mouth movement (Tate et al., 2014; Chang et al., 2017; Nakai et al., 2017). High-gamma augmentation in the STG immediately following the onset of overt response may reflect self-monitoring of own voice (Schulz et al., 2005).

Picture naming-related high-gamma augmentation sequentially involving the bilateral occipital to posterior fusiform regions likely reflects lower- to higher-order visual processing (Fisch et al., 2009). Previous studies reported that electrical stimulation of the medial/polar surface of the occipital lobe on either hemisphere frequently induced the perception of phosphene, whereas that of the posterior fusiform gyrus occasionally induced the perception of visual distortion (Lee et al., 2000; Nakai et al., 2017). Stimulation of the left posterior fusiform gyrus was also reported to be associated with transient impairment of visual semantic recognition (Forseth et al., 2018).

The left frontal-parietal-temporal perisylvian network regions consisting of the left MTG, SMG, and IFG showed high-gamma augmentation preferentially during the auditory naming task, whereas the occipital-fusiform regions showed high-gamma augmentation preferentially during picture naming task. This observation is consistent with previous fMRI and iEEG studies of English-speaking patients (Hamberger et al., 2014; Nakai et al., 2019). Our results support the notion that picture naming task, compared to auditory naming, can be completed with less extensive activation of the left frontal-parietal-temporal perisylvian network but requires more extensive activation of the ventral visual pathways. Less extensive high-gamma augmentation in the left inferior-frontal region during picture naming task can be explained in part by the difference in experimental paradigms. Not picture- but auditory-naming task requires syntactic processing, which is partly supported by the left inferior-frontal gyrus (Dapretto and Bookheimer, 1999; Hagoort, 2005). Further studies are warranted to determine whether the extent of high-gamma augmentation in the left frontal-parietal-temporal perisylvian network is dependent on the modality of stimuli or the relative requirement of syntactic processing in auditory naming versus picture naming.

4.2. Feasibility of multicenter collaborative studies across the Eastern and Western hemispheres

iEEG recording provides a unique window to measure neural dynamics with outstanding signal fidelity, temporal resolution of the order of 10 ms, and spatial resolution of 5–10 mm (Ball et al.,

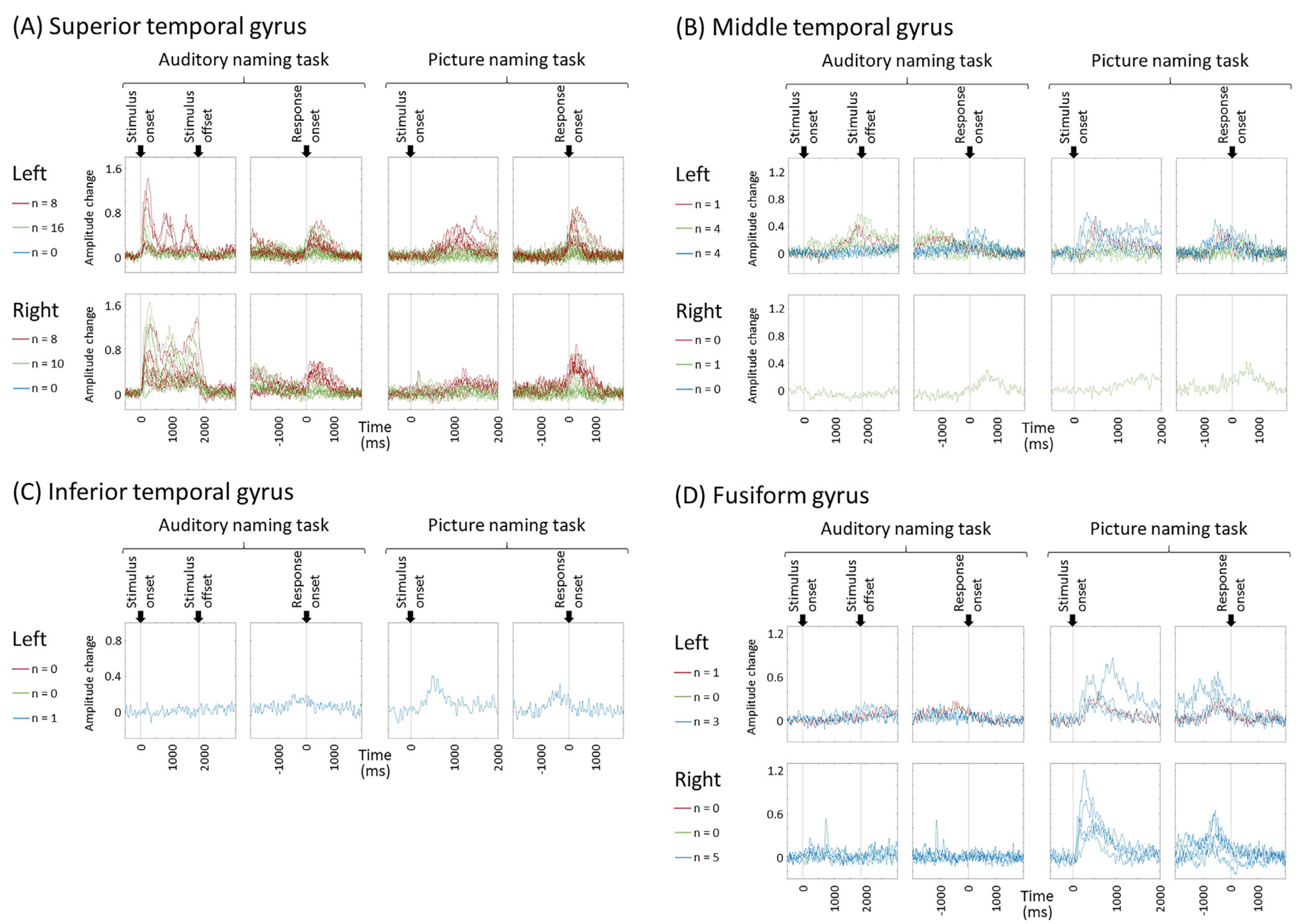

Fig. 3. Naming-related high-gamma modulations at a group level. Percent change of high-gamma amplitude at channels showing significant augmentation (Table 2) plotted as a function of time. Red lines: significant high-gamma augmentation during both naming tasks. Green lines: significant high-gamma augmentation during auditory naming task alone. Blue lines: significant high-gamma augmentation during picture naming task alone. "n" indicates the number of electrodes from each category included in the plot. Electrode sites failing to show significant high-gamma augmentation are not presented in these figures. (A) Superior temporal gyrus (STG). (B) Middle temporal gyrus (MTG). (C) Inferior temporal gyrus (ITG). (D) Fusiform gyrus. (E) Occipital lobe. (F) Supramarginal gyrus (SMG). (G) Inferior frontal gyrus (IFG). (H) Inferior precentral gyrus (iPreCG), defined as the precentral gyrus between the level of superior-frontal and lateral sulci. (I) Inferior postcentral gyrus (iPostCG), defined as the postcentral gyrus between the level of superior-frontal and lateral sulci. (For interpretation of the references to colour in this figure legend, the reader is referred to the web version of this article.)

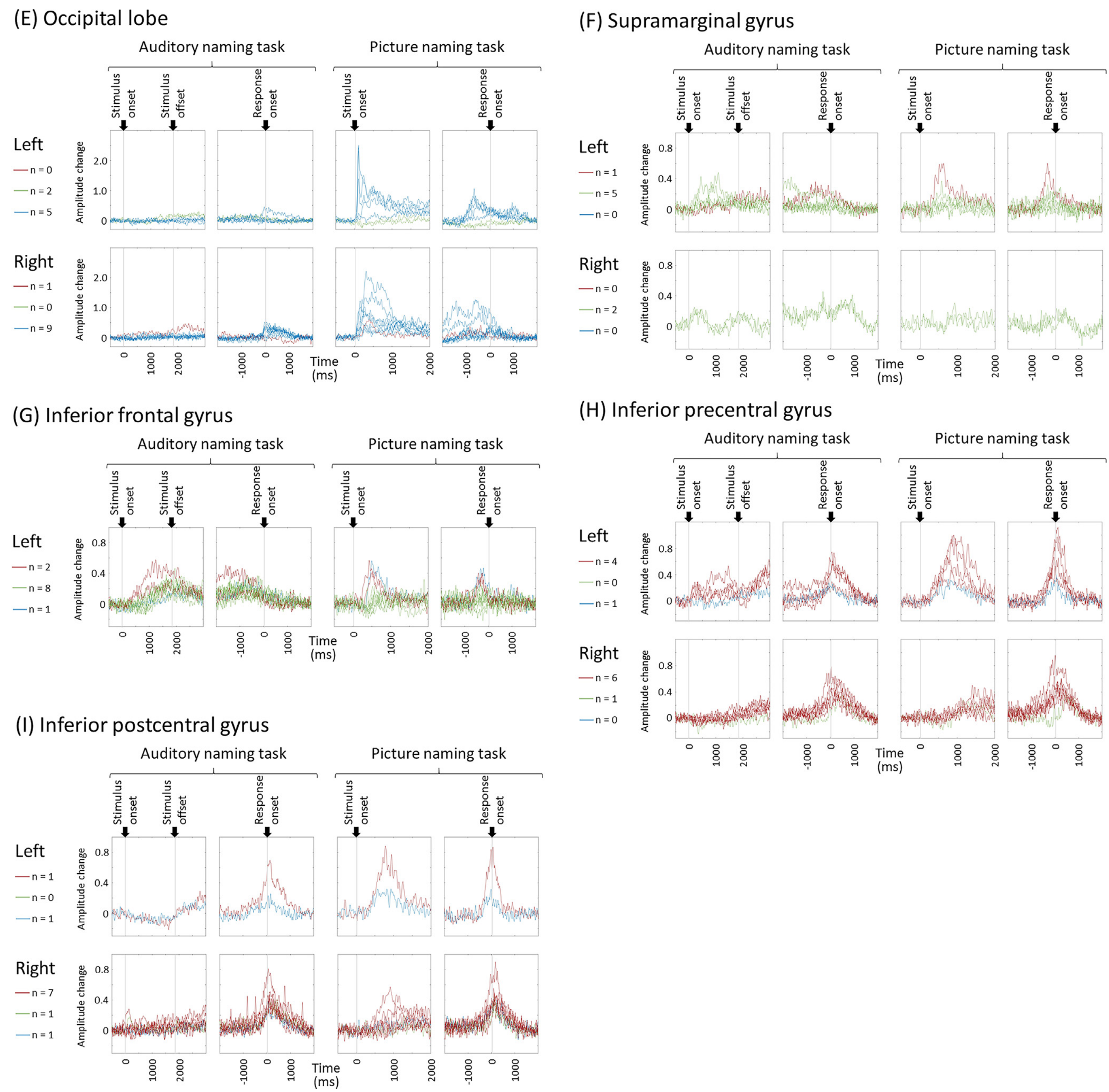

Fig. 3 (*continued*)

2009). Investigators often have difficulty in securing sufficient statistical power because the number of extraoperative iEEG recording is typically less than 30 per year in many of tertiary epilepsy centers. Thus, multicenter collaborative studies have been employed across countries to address research questions of interest promptly and also to increase the generalizability of models of normal and pathological physiology (e.g., Frauscher et al., 2018; Jacobs et al., 2018). One concern for transnational collaborative studies on culturally-defined behaviors, such as language, is that the underlying physiology may differ, thus presenting challenges for pooling data. However, based on the results of this study, we believe that multicenter studies utilizing iEEG-based language mapping for clinical and cognitive research are feasible across Eastern and Western hemispheres. We strongly encourage the development of multi-language studies as the majority of iEEG-based language research has reflected the English language, whereas 80% of the general population in the world primarily speak languages other than English (McArthur, 2004). Further study is warranted to determine if the differences in syntax and semantics between languages such as English and Japanese have a substantial influence on the spatiotemporal dynamics of neurological systems which support language.

A potential pitfall for intercontinental studies includes regional differences in the frequency of alternating current used in electrical infrastructure. iEEG signals suffer from contamination due to line noise at 50-Hz or 60-Hz depending on the region in which the recording is made. This is of critical importance for iEEG studies as a primary variable of interest is event-related augmentation of recorded neurological activity in a broad frequency range above 50 Hz (Brown et al., 2008; Towle et al., 2008; Manning et al.,

Table 2
Spatial profiles of high-gamma augmentation.

	Number of all available channels	Number of channels showing significant HG augmentation during both naming tasks (%)	Number of channels showing significant HG augmentation during auditory naming task alone (%)	Number of channels showing significant HG augmentation during picture naming task alone (%)
Left STG	49	8 (16.3)	16 (32.7)	0 (0.0)
Right STG	59	8 (13.6)	10 (16.9)	0 (0.0)
Left MTG	91	1 (1.1)	4 (4.4)	4 (4.4)
Right MTG	49	0 (0.0)	1 (2.0)	0 (0.0)
Left ITG	25	0 (0.0)	0 (0.0)	1 (4.0)
Right ITG	14	0 (0.0)	0 (0.0)	0 (0.0)
Left fusiform	12	1 (8.3)	0 (0.0)	3 (25.0)
Right fusiform	12	0 (0.0)	0 (0.0)	5 (41.7)
Left occipital	11	0 (0.0)	2 (18.2)	5 (45.5)
Right occipital	21	1 (4.8)	0 (0.0)	9 (42.9)
Left SMG	15	1 (6.7)	5 (33.3)	0 (0.0)
Right SMG	25	0 (0.0)	2 (8.0)	0 (0.0)
Left IFG	28	2 (7.1)	8 (28.6)	1 (3.6)
Right IFG	28	0 (0.0)	0 (0.0)	0 (0.0)
Left iPreCG	6	4 (66.7)	0 (0.0)	1 (16.7)
Right iPreCG	12	6 (50.0)	1 (8.3)	0 (0.0)
Left iPostCG	2	1 (50.0)	0 (0.0)	1 (50.0)
Right iPostCG	18	7 (38.9)	1 (5.6)	1 (5.6)

STG: superior-temporal gyrus. MTG: middle-temporal gyrus. ITG: inferior-temporal gyrus.
SMG: supra-marginal gyrus. IFG: inferior-frontal gyrus. iPreCG: inferior precentral gyrus.
iPostCG: inferior postcentral gyrus. HG: high-gamma.

2009; Crone et al., 2011). In the present study, we defined the frequency range of high-gamma activity as 65–95 Hz. This frequency range effectively avoids potential contamination of 50-Hz or 60-Hz line noise (as well as those of related harmonic frequencies), thereby maximizing the potential to relate our findings to those from other laboratories independent of geographical region.

To facilitate multi-language auditory naming studies, we have made standardized auditory sentence stimuli publicly available in English, Hindi, Arabic, and Japanese (https://www.ncbi.nlm.nih.gov/pmc/articles/PMC5744878/; Kambara et al., 2018b). Additional language releases are planned and in development.

4.3. Limitations of the study

The main limitation of the present study is the small sample size. As a result, we did not have complete coverage of all brain regions. While we have demonstrated the involvement of several frontal, temporal, and occipital regions in auditory and picture naming, these networks may include other regions which were not sampled in the present study. We plan to continue to measure naming-related high-gamma activity during extraoperative iEEG recordings in all languages, but due to the slow rate at which such recordings occur, several years would be needed to accumulate a sufficient sample size to detect a difference in neural dynamics between two patient cohorts speaking two distinct languages. This difficulty may be ameliorated in the future by increased multicenter studies. Furthermore, we did not determine the association between naming-related high-gamma activity and stimulation-induced behavioral changes, since ESM was not systematically employed in our study cohort and meaningful analysis was not possible to conduct.

Another limitation of this study is the lack of direct comparison of high-gamma measures between age-matched cohorts of Japanese- and English-speaking patients. The median age of Japanese-speaking patients was 33.3 years in the present study, but 14.0 years in a previous iEEG study of 79 English-speaking patients (Nakai et al., 2019). A sophisticated statistical analysis controlling the potential effects of epilepsy profiles (e.g., mixed model analysis as reported in Nakai et al., 2018) may be warranted to employ in larger cohorts of patients for optimal determination of the effect of spoken native language on the spatiotemporal dynamics of naming-related high-gamma activity.

Conflict of interest

None of the authors have potential conflicts of interest to be disclosed.

Acknowledgments

This work was supported by (1) Intramural Research Grant (28-4: Clinical Research for Diagnostic and Therapeutic Innovations in Developmental Disorders) from Neurological and Psychiatric Disorders of National Center of Neurology and Psychiatry, Japan, and (2) NIH grant NS064033, USA. We are grateful to Ms. Satsuki Konno at National Center Hospital, National Center of Neurology and Psychiatry for the collaboration and assistance in performing the studies described above.

Appendix A. Supplementary material

Supplementary data to this article can be found online at https://doi.org/10.1016/j.clinph.2019.04.008.

References

Arya R, Wilson JA, Fujiwara H, Rozhkov L, Leach JL, Byars AW, et al. Presurgical language localization with visual naming associated ECoG high- gamma modulation in pediatric drug-resistant epilepsy. Epilepsia 2017;58:663–73.
Arya R, Horn PS, Crone NE. ECoG high-gamma modulation versus electrical stimulation for presurgical language mapping. Epilepsy Behav 2018;79:26–33.
Austermuehle A, Cocjin J, Reynolds R, Agrawal S, Sepeta L, Gaillard WD, et al. Language functional MRI and direct cortical stimulation in epilepsy preoperative planning. Ann Neurol 2017;81:526–37.
Babajani-Feremi A, Holder CM, Narayana S, Fulton SP, Choudhri AF, Boop FA, et al. Predicting postoperative language outcome using presurgical fMRI, MEG, TMS, and high gamma ECoG. Clin Neurophysiol 2018;129:560–71.
Baddeley A. The episodic buffer: a new component of working memory? Trends Cogn Sci 2000;4:417–23.
Ball T, Kern M, Mutschler I, Aertsen A, Schulze-Bonhage A. Signal quality of simultaneously recorded invasive and non-invasive EEG. Neuroimage 2009;46:708–16.
Bauer PR, Vansteensel MJ, Bleichner MG, Hermes D, Ferrier CH, Aarnoutse EJ, et al. Mismatch between electrocortical stimulation and electrocorticography frequency mapping of language. Brain Stimul 2013;6:524–31.

Binder JR, Frost JA, Hammeke TA, Cox RW, Rao SM, Prieto T. Human brain language areas identified by functional magnetic resonance imaging. J Neurosci 1997;17:353–62.
Brown EC, Rothermel R, Nishida M, Juhász C, Muzik O, Hoechstetter K, et al. In vivo animation of auditory-language-induced gamma-oscillations in children with intractable focal epilepsy. Neuroimage 2008;41:1120–31.
Budke M, Avecillas-Chasin JM, Villarejo F. Implantation of depth electrodes in children using VarioGuide® frameless navigation system: technical note. Open Neurosurg 2018;15:302–9.
Catani M, Mesulam M. The arcuate fasciculus and the disconnection theme in language and aphasia: history and current state. Cortex 2008;44:953–61.
Cervenka MC, Corines J, Boatman-Reich DF, Eloyan A, Sheng X, Franaszczuk PJ, et al. Electrocorticographic functional mapping identifies human cortex critical for auditory and visual naming. Neuroimage 2013;69:267–76.
Chang EF, Breshears JD, Raygor KP, Lau D, Molinaro AM, Berger MS. Stereotactic probability and variability of speech arrest and anomia sites during stimulation mapping of the language dominant hemisphere. J Neurosurg 2017;126:114–21.
Cook V. Second language learning and language teaching. New York: Routledge; 2016.
Crone NE, Korzeniewska A, Franaszczuk PJ. Cortical γ responses: searching high and low. Int J Psychophysiol 2011;79:9–15.
Dapretto M, Bookheimer SY. Form and content: dissociating syntax and semantics in sentence comprehension. Neuron 1999;24:427–32.
Démonet JF, Chollet F, Ramsay S, Cardebat D, Nespoulous JL, Wise R, et al. The anatomy of phonological and semantic processing in normal subjects. Brain 1992;115:1753–68.
Edwards E, Nagarajan SS, Dalal SS, Canolty RT, Kirsch HE, Barbaro NM, et al. Spatiotemporal imaging of cortical activation during verb generation and picture naming. Neuroimage 2010;50:291–301.
Fisch L, Privman E, Ramot M, Harel M, Nir Y, Kipervasser S, et al. Neural "ignition": enhanced activation linked to perceptual awareness in human ventral stream visual cortex. Neuron 2009;64:562–74.
Forseth KJ, Kadipasaoglu CM, Conner CR, Hickok G, Knight RT, Tandon N. A lexical semantic hub for heteromodal naming in middle fusiform gyrus. Brain 2018;141:2112–26.
Frauscher B, von Ellenrieder N, Zelmann R, Rogers C, Nguyen DK, Kahane P, et al. High-frequency oscillations in the normal human brain. Ann Neurol 2018;84:374–85.
Hagoort P. On Broca, brain, and binding: a new framework. Trends Cogn Sci 2005;9:416–23.
Hamberger MJ, Seidel WT. Auditory and visual naming tests: normative and patient data for accuracy, response time, and tip-of-the-tongue. J Int Neuropsychol Soc 2003;9:479–89.
Hamberger MJ, Habeck CG, Pantazatos SP, Williams AC, Hirsch J. Shared space, separate processes: neural activation patterns for auditory description and visual object naming in healthy adults. Hum Brain Mapp 2014;35:2507–20.
Hickok G, Poeppel D. The cortical organization of speech processing. Nat Rev Neurosci 2007;8:393–402.
Hoechstetter K, Bornfleth H, Weckesser D, Ille N, Berg P, Scherg M. BESA source coherence: a new method to study cortical oscillatory coupling. Brain Topogr 2004;16:233–8.
Hongo J. Japan ranks 40th of 48 countries in TOEIC scores. Wall Street J 2014.
Jacobs J, Wu JY, Perucca P, Zelmann R, Mader M, Dubeau F, et al. Removing high-frequency oscillations: a prospective multicenter study on seizure outcome. Neurology 2018;91:e1040–52.
Kambara T, Brown EC, Silverstein BH, Nakai Y, Asano E. Neural dynamics of verbal working memory in auditory description naming. Sci Rep 2018a;8:15868.
Kambara T, Sood S, Alqatan Z, Klingert C, Ratnam D, Hayakawa A, et al. Presurgical language mapping using event-related high-gamma activity: the Detroit procedure. Clin Neurophysiol 2018b;129:145–54.
Keller CJ, Bickel S, Honey CJ, Groppe DM, Entz L, Craddock RC, et al. Neurophysiological investigation of spontaneous correlated and anticorrelated fluctuations of the BOLD signal. J Neurosci 2013;33:6333–42.
Koga S, Rothermel R, Juhász C, Nagasawa T, Sood S, Asano E. Electrocorticographic correlates of cognitive control in a Stroop task-intracranial recording in epileptic patients. Hum Brain Mapp 2011;32:1580–91.
Kojima K, Brown EC, Rothermel R, Carlson A, Fuerst D, Matsuzaki N, et al. Clinical significance and developmental changes of auditory-language-related gamma activity. Clin Neurophysiol 2013a;124:857–69.
Kojima K, Brown EC, Matsuzaki N, Asano E. Animal category-preferential gamma-band responses in the lower- and higher-order visual areas: intracranial recording in children. Clin Neurophysiol 2013b;124:2368–77.
Kunii N, Kamada K, Ota T, Greenblatt RE, Kawai K, Saito N. The dynamics of language-related high-gamma activity assessed on a spatially-normalized brain. Clin Neurophysiol 2013;124:91–100.
Lachaux JP, Fonlupt P, Kahane P, Minotti L, Hoffmann D, Bertrand O, et al. Relationship between task-related gamma oscillations and BOLD signal: new insights from combined fMRI and intracranial EEG. Hum Brain Mapp 2007;28:1368–75.
Lee HW, Hong SB, Seo DW, Tae WS, Hong SC. Mapping of functional organization in human visual cortex: electrical cortical stimulation. Neurology 2000;54:849–54.
Lehmann WP. A structural principle of language and its implications. Language 1973;49:47–66.
Lesser RP, Crone NE, Webber WRS. Subdural electrodes. Clin Neurophysiol 2010;121:1376–92.
Lin J, Zuo H, Hong B, He J, Jin Z, Zhang G, et al. Mapping language area in the frontal lobe of the left-dominant hemisphere with high gamma electrocorticography. J Neurolinguistics 2015;35:85–95.
Llorens A, Trébuchon A, Liégeois-Chauvel C, Alario FX. Intra-cranial recordings of brain activity during language production. Front Psychol 2011;2:375.
Manning JR, Jacobs J, Fried I, Kahana MJ. Broadband shifts in local field potential power spectra are correlated with single-neuron spiking in humans. J Neurosci 2009;29:13613–20.
Martino J, De Witt Hamer PC, Berger MS, Lawton MT, Arnold CM, de Lucas EM, et al. Analysis of the subcomponents and cortical terminations of the perisylvian superior longitudinal fasciculus: a fiber dissection and DTI tractography study. Brain Struct Funct 2013;218:105–21.
Matsumoto R, Nair DR, LaPresto E, Najm I, Bingaman W, Shibasaki H, et al. Functional connectivity in the human language system: a cortico-cortical evoked potential study. Brain 2004;127:2316–30.
Matsumoto R, Nair DR, Ikeda A, Fumuro T, Lapresto E, Mikuni N, et al. Parieto-frontal network in humans studied by cortico-cortical evoked potential. Hum Brain Mapp 2012;33:2856–72.
McArthur T. Is it world or international or global English, and does it matter? English Today 2004;20:3–15.
Mooij AH, Huiskamp GJM, Gosselaar PH, Ferrier CH. Electrocorticographic language mapping with a listening task consisting of alternating speech and music phrases. Clin Neurophysiol 2016;127:1113–9.
Nagasawa T, Matsuzaki N, Juhász C, Hanazawa A, Shah A, Mittal S, et al. Occipital gamma-oscillations modulated during eye movement tasks: simultaneous eye tracking and electrocorticography recording in epileptic patients. Neuroimage 2011;58:1101–9.
Nakai Y, Jeong JW, Brown EC, Rothermel R, Kojima K, Kambara T, et al. Three- and four-dimensional mapping of speech and language in patients with epilepsy. Brain 2017;140:1351–70.
Nakai Y, Nagashima A, Hayakawa A, Osuki T, Jeong JW, Sugiura A, et al. Four-dimensional map of the human early visual system. Clin Neurophysiol 2018;129:188–97.
Nakai Y, Sugiura A, Brown EC, Sonoda M, Jeong JW, Rothermel R, et al. Four-dimensional functional cortical maps of visual and auditory language: intracranial recording. Epilepsia 2019;60:255–67.
Nishida M, Korzeniewska A, Crone NE, Toyoda G, Nakai Y, Ofen N, et al. Brain network dynamics in the human articulatory loop. Clin Neurophysiol 2017;128:1473–87.
Ogawa H, Kamada K, Kapeller C, Prueckl R, Takeuchi F, Hiroshima S, et al. Clinical impact and implication of real-time oscillation analysis for language mapping. World Neurosurg 2017;97:123–31.
Papp N, Ktonas P. Critical evaluation of complex demodulation techniques for the quantification of bioelectrical activity. Biomed Sci Instrum 1977;13:135–45.
Ray S, Crone NE, Niebur E, Franaszczuk PJ, Hsiao SS. Neural correlates of high-gamma oscillations (60–200 Hz) in macaque local field potentials and their potential implications in electrocorticography. J Neurosci 2008;28:11526–36.
Ruescher J, Iljina O, Altenmüller DM, Aertsen A, Schulze-Bonhage A, Ball T. Somatotopic mapping of natural upper- and lower-extremity movements and speech production with high gamma electrocorticography. Neuroimage 2013;81:164–77.
Sanai N, Mirzadeh Z, Berger MS. Functional outcome after language mapping for glioma resection. N Engl J Med 2008;358:18–27.
Schulz GM, Varga M, Jeffires K, Ludlow CL, Braun AR. Functional neuroanatomy of human vocalization: an H215O PET study. Cereb Cortex 2005;15:1835–47.
Sinai A, Bowers CW, Crainiceanu CM, Boatman D, Gordon B, Lesser RP, et al. Electrocorticographic high gamma activity versus electrical cortical stimulation mapping of naming. Brain 2005;128:1556–70.
Tanji K, Suzuki K, Delorme A, Shamoto H, Nakasato N. High-frequency gamma-band activity in the basal temporal cortex during picture-naming and lexical-decision tasks. J Neurosci 2005;25:3287–93.
Tate MC, Herbet G, Moritz-Gasser S, Tate JE, Duffau H. Probabilistic map of critical functional regions of the human cerebral cortex: Broca's area revisited. Brain 2014;137:2773–82.
Teruya K. Grammar as a resource for the construction of language logic for advanced language learning in Japanese. In: Byrnes H, editor. Advanced language learning: The contribution of Halliday and Vygotsky. London: Continuum; 2006. p. 109–33.
Towle VL, Yoon HA, Castelle M, Edgar JC, Biassou NM, Frim DM, et al. ECoG gamma activity during a language task: differentiating expressive and receptive speech areas. Brain 2008;131:2013–27.
Wen J, Yu T, Li Y, Li X. Using electrocorticography for presurgical language mapping in epilepsy patients. J Clin Neurosci 2017;44:320–2.
Wickens DD. Encoding categories of words: an empirical approach to meaning. Psychological Rev 1970;77:1–15.
Xiang HD, Fonteijn HM, Norris DG, Hagoort P. Topographical functional connectivity pattern in the perisylvian language networks. Cereb Cortex 2010;20:549–60.